UNIVERSITI TEKNOLOGI MARA

Journal of Mechanical Engineering

An International Journal

Volume 10 No. 2 December 2013 ISSN 1823-5514

JOURNAL OF MECHANICAL ENGINEERING (JMechE)

Journal of Mechanical Engineering (ISSN 1823-5514) is published by the Faculty of Mechanical Engineering (FKM) and UiTM Press, Universiti Teknologi MARA, 40450 Shah Alam, Selangor, Malaysia.

Journal of Mechanical Engineering

An International Journal

Volume 10 No. 2 **December 2013** **ISSN 1823-5514**

Material Characterization and Axial Crushing Tests of Single and Double-Walled Columns at Intermediate Strain Rates

Leonardo Gunawan
Sahril Afandi Sitompul
Tatacipta Dirgantara
Ichsan Setya Putra
Light-weight Structures Research Group
Faculty of Mechanical and Aerospace Engineering
Institut Teknologi Bandung, Indonesia

Hoon Huh
Computational Solid Mechanics and Design Laboratory Korea Advanced Institute of Science and Technology, Republic of Korea

ABSTRACT

This paper presents results of dynamic tensile tests of the St37 mild steel and dynamic axial impact tests of columns made of the same material. Both tests were performed in conjunction with the validation of numerical simulations of dynamic crushing of single and double-walled square columns. The tensile tests, which were performed at several strain-rates ranging from $0.001s^{-1}$ to $100s^{-1}$, provided the plastic flow stress data of the St37 mild steel that increases as the strain-rate increases. The dynamic axial crushing tests were conducted to single and double-walled square columns made of the St37 mild steel. The test results indicate that the double-walled column has higher mean crushing force and larger energy absorbing capability than those of single-walled columns. Finite element simulations of the dynamic impact tests employing the flow stress data obtained from the tensile tests are in good agreements with those from the experiments. It is noted that the use of the strain-rate dependent material model of the St37 material improved the accuracy of the numerical simulations.

Keywords: *Dynamic tensile test, strain-rate dependent material properties, dynamic axial crushing, single-walled column, double-walled column.*

ISSN 1823-5514

Introduction

Thin-walled metal columns are conventional energy absorbing devices which have been applied in various structures, such as frame structures of land and railway vehicles. The columns are designed to absorb the collision energy through an axial progressive collapse mechanism and to prevent excessive deceleration levels in order to protect the passengers [1].

Fundamental theoretical studies on the mechanics of thin-walled structures were reported by Alexander [2], Wierzbicki & Abramowicz [3, 4], and Andrews et al. [5]. In those studies, plastic collapses of thin-walled columns with different cross section were studied and the relationships between column geometry, axial crushing force, and impact energy absorption characteristics for different folding modes were derived. Some experimental works were carried out to validate the theoretical results.

Following the theoretical studies, a large number of numerical investigations on the crushing behavior of thin-walled columns were carried out. The crushing behavior of square thin-walled aluminum extrusions subjected to axial loading was investigated by Abramowicz and Wierzbicki [6], and Langseth and Hopperstad [7]. More recently, numerical simulations of thin-walled columns of various materials and cross-sections were reported by Langseth et al. [8, 9], Sun and Osire [10], Rossi et al.[11], and Zhang and Huh [12]. Tarigopula et al. [13, 14], Aljawi et al.[15], Zhang et al.[16], and Song et al.[17] conducted numerical simulations validated with experimental data.

The numerical investigations on the crushing behavior of thin-walled columns require material data that describes the dependency of the material mechanical properties to the strain-rate. Huh [18] investigated the effect of the strain-rate on the stress-strain curves and the failure elongation for several steel sheets for auto-body at room temperature. The study was carried out at the strain-rates in the real auto-body crash, ranging from 0.003 s^{-1} to 200 s^{-1}. For this study, a servo-hydraulic type high speed material testing machine was developed. Recently, Huh [19] reported an experimental study to obtain both the strain-rate and the temperature dependent stress-strain curves of steel sheets for an auto-body.

Experimental investigations on the crushing behavior of thin-walled columns are carried out to understand the physical phenomena and to validate results of theoretical and numerical investigations. Yuen et al.[20] reported experimental works on the quasi-static and dynamic crushing behaviour of single-walled and double-walled mild steel columns with seven double-walled configurations combining square and circular columns. The tests were carried out in order to find the highest energy absorption characteristics.

Jusuf et al. [21] reported computational works which were carried out to evaluate the effects of inserting an inner column into a outer column to form a double-walled column. Comparisons of mean crushing forces, specific

energy absorptions, and crush force efficiencies between the single and the double thin-walled columns were presented for several different configurations of double-walled columns. In conjunction with the computational works, two experimental works were conducted. The first is the tensile tests of St37 mild steel to obtain its mechanical properties at several strain-rates ranging from 0.001 s^{-1} to 100 s^{-1}. The second is the dynamic axial crushing tests of single and double-walled square columns to obtain their crushing forces data. This paper presents and discusses results of the two experimental works.

Tensile Test

Dynamic tensile tests of steel sheets are aimed to provide the data of mechanical properties at several strain-rates that is needed for impact simulations. Each test involved the measurement of the length change of a specimen and the loading force associated with it. The measurement of strain at high strain-rates is more difficult than that at a quasi-static condition. Extensometer that is usually used at the quasi-static measurement can not be used since it does not have good response characteristics at high strain-rates. A non-contacting strain measurement device such as an optical or a laser extensometer is more suitable for this purpose. A load cell is used to measure the loading force. For the test at the quasi-static condition, the load cell is considered to deform uniformly. However, at higher strain-rates, the test duration is short and there is not enough time for the load cell to have uniform elastic deformation. This makes the measurement of forces at higher strain-rates test different from those at the quasi-static test condition.

The tensile test principally can be carried out using any machine which can apply a uniaxial tensile load to a specimen to failure at a specified high strain-rate with a constant load, or an instant load wave for very high strain-rate. The machine should be able to measure main test parameters such as displacement, strain and load. Three type of testing systems, in general, are required for the measurements at the strain-rate range of important to crashworthiness, i.e. from 1 s^{-1} to 1000 s^{-1}. The conventional load frame can be used for quasi-static testing; the servo hydraulic type machine can be used for strain-rates between 0.1 s^{-1} and 500 s^{-1}; and the bar type machine can be used for strain-rates between 100 s^{-1} and 1000 s^{-1} or higher [22].

The tensile tests were carried out at the Computational Solid Mechanics and Design Laboratory at Korea Advanced Institute of Science and Technology (CSMD Laboratory – KAIST). The quasi-static tensile tests were performed by using the Instron 5583 universal testing machine. The crosshead of the machine can move with speeds between 0.05 and 500 mm/min. The maximum tension force of the machine is 150 kN for crosshead speed up to 50 mm/min, and 25 kN for crosshead speed up to 500 mm/min. Dynamic tensile tests were performed

by using a high speed material testing machine of the servo-hydraulic type, as shown in Figure 1, to obtain the mechanical properties at the intermediate strain-rates. The machine has a maximum stroke velocity of 7800 mm/s, a maximum load of 30 kN, and a maximum displacement of 300 mm. The tension force is measured by a specially designed piezo electric loadcell. The displacement of the specimen is measured by using linear displacement transducer (LVDT) from Sentech Company. The machine has been carefully calibrated for its displacement and load measurement system. The repeatability of its measurement results has also been verified [18, 19].

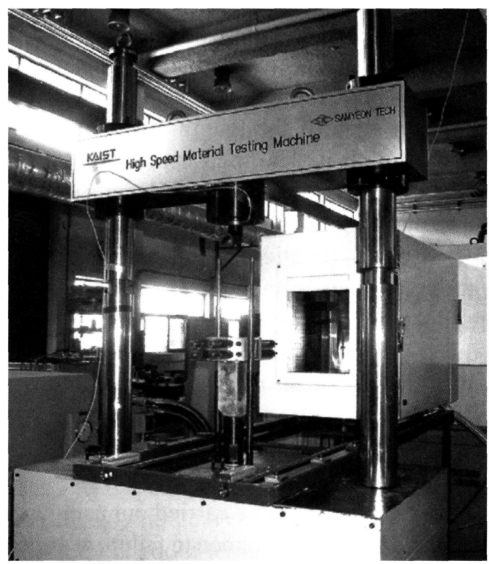

Figure 1. High speed material testing machine [18]

Specimen

The major geometry parameters of all tensile specimens are the length (L) and the width of the parallel region, the gauge length (G), and the radius of the fillet (R), as shown in Figure 2. The values of those parameters were adopted from the results of the study by Huh [18], in which several specimens with varying L and G were analyzed using finite element method and verified using experiments. The study ensured that the specimens would have uniform strain distribution in the gauge section during the test.

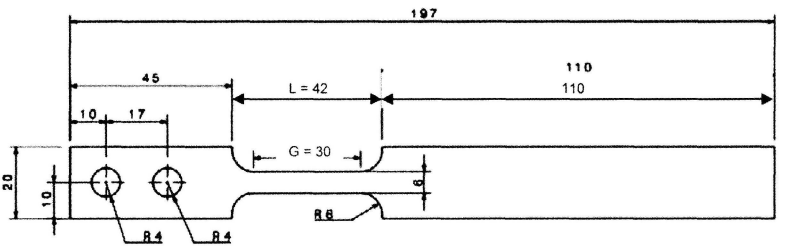

Figure 2. Dimensions of the tensile test specimen (in mm)

Results of Quasi-static Tensile Tests

The quasi-static tensile tests were carried out at strain-rates of 0.001 s^{-1} and 0.01 s^{-1}. With the specimen gauge length of 30 mm, the speeds of the head were 0.03 mm/s (1.8 mm/min) and 0.3 mm/s (18 mm/min). Figure 3 shows the results of the quasi-static tensile tests as curves of engineering stress vs engineering strain. The data were then analyzed to obtain the Young's modulus (E), ultimate strength (σ_u) and yield strength (σ_y) by using 0.2% offset, as shown in Figure 4. At both strain-rates, E = 195 GPa, which is within the range of E for steel (190–210 GPa). At the strain-rate of 0.001 s^{-1}, σ_y = 197 MPa and σ_u = 298 MPa, whereas at the strain-rate of 0.01 s^{-1}, σ_y = 209 MPa and σ_u = 300 MPa. The measured strengths are lower than those found in datasheet of the St37 (σ_y = 235 MPa, σ_u = 360–510 MPa). From the engineering stress vs engineering strain data, the true stress vs effective plastic strain curves were determined, as shown in Figure 5.

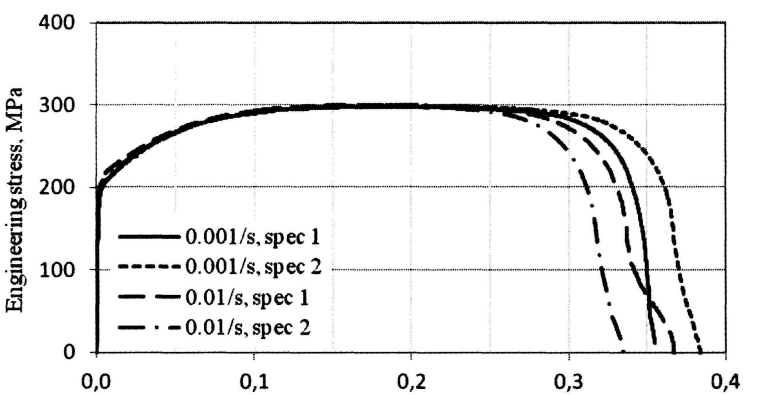

Figure 3. Stress vs strain curves obtained from quasi-static tensile testing machine at strain-rate of 0.001 s^{-1} and 0.01 s^{-1}

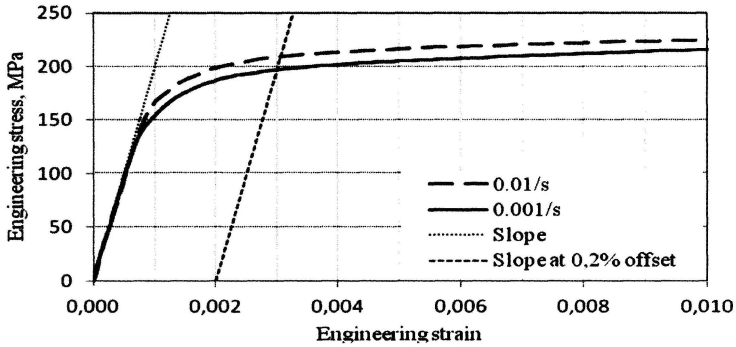

Figure 4. Determination of Young's modulus and yield strengths

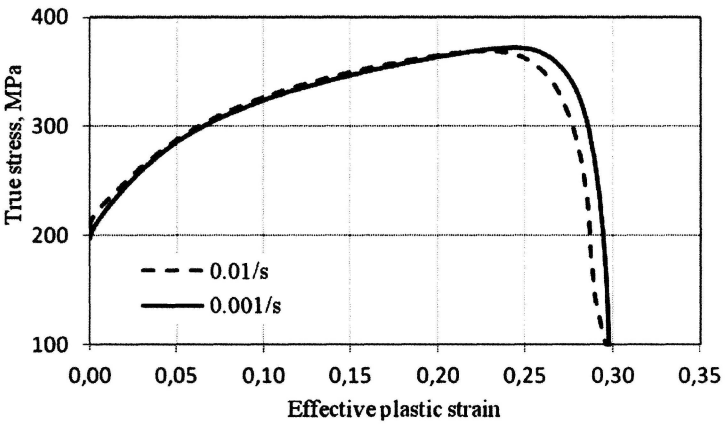

Figure 5. True stress vs effective plastic strain curves of St37 mild steel measured at strain-rates of 0.001 s^{-1} and 0.01 s^{-1}

Results of Dynamic Tensile Tests

The dynamic tensile tests were carried out at strain-rates of 0.1 s^{-1}, 1 s^{-1}, 10 s^{-1} and 100 s^{-1}. With the specimen gauge length of 30 mm, they correspond to stroke velocities of 3 mm/s, 30 mm/s, 300 mm/s, and 3000 mm/s. For each strain-rate, 5 specimens were tested and the data were then averaged. Data obtained from the dynamic tensile tests are principally similar to those obtained from the quasi-static tensile tests. However, due to the load-ringing phenomenon, the measured displacements and forces data oscillated. The displacements and forces data were then smoothed, from which the force vs displacement curves were constructed. Figure 6 shows the displacements and forces data of a specimen measured at strain-rate of 0.1 s^{-1}.

For the dynamic tensile tests, the calculations of engineering strains were carried out by implementing engineering strain ratio of 0.935, the ratio between the engineering strain of the local displacement at the gauge section to that obtained from the overall displacement of the crosshead [18]. The true stress vs effective plastic strain curves were then constructed by following the procedure described in the quasi-static test. The results are shown in Figure 7.

Figure 8 shows the true stress vs effective plastic strain curves measured using dynamic tensile tests combined with those obtained using quasi-static tensile tests. The data is presented up to the ultimate strengths of the material.

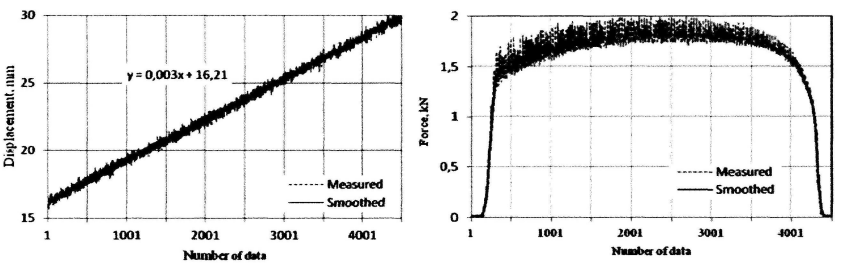

(a) (b)

Figure 6. (a) Displacements and (b) forces data from dynamic tensile test at strain-rate of 0.1 s^{-1}

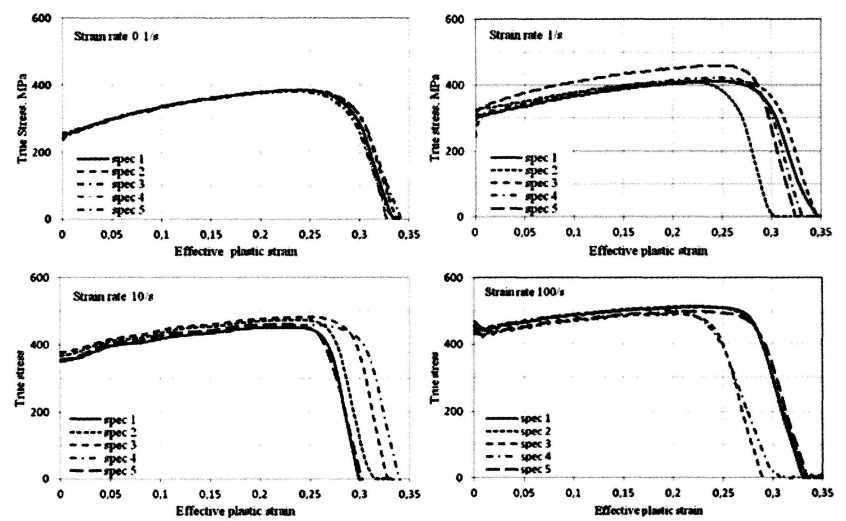

Figure 7. Stress vs strain curves of St37 mild steel measured at strain-rates of 0.1 s^{-1}, 1 s^{-1}, 10 s^{-1} and 100 s^{-1}

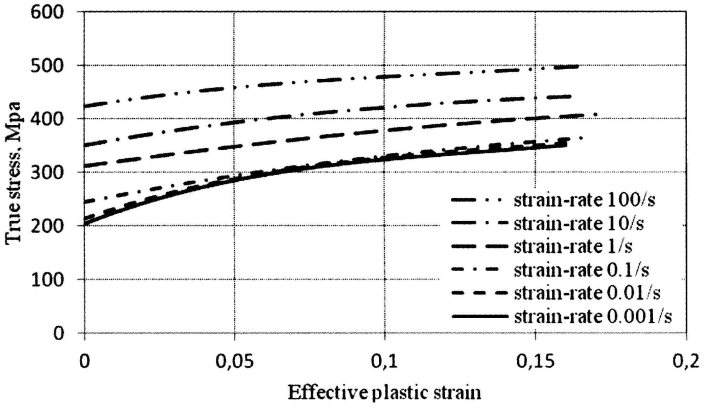

Figure 8. Stress vs strain curves of the St37 mild steel at several strain-rates

It can be seen that the yield and ultimate strengths of the material increase at higher strain-rates.

In the material model of the finite element analysis, the measured strain-rate sensitive material data was used directly. This method has a limitation, that if data at higher or lower strain-rates than those available are needed, then the values at maximum or minimum strain-rates will be used. Alternatively, the data can be entered using one of the material models such as Johnson-Cook, Cowper-Symonds, etc. By using the material model, stress values at strain-rates beyond the measurement range can be predicted.

Dynamic Axial Crushing Tests

High Speed Crash Testing Machine

The High-Speed Crash Testing Machine (HSCTM) owned by the CSMD KAIST was used to evaluate the crushing forces and the deformation modes of the crash box specimens. The HSCTM is 10,000 mm long and 1,400 mm wide as shown in Figure 9 [23]. It comprises five major parts: a carrier; a hydraulic unit which triggers the carrier; a rail; a clamp for mounting the specimen; and a damper for the shock-absorption of excess energy. The hydraulic unit can move the 290 kg carrier along the rail to crash the specimen with a maximum speed of 21 m/s.

Measurement and Data Processing System

During the test, the specimen was held using a 25 mm thick clamp support made of steel. The clamp support was mounted to the load cell of the testing machine. The specimen was then crushed axially at the free end by the carrier.

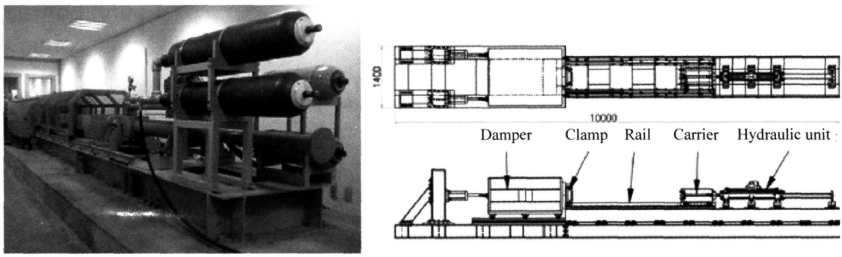

Figure 9. The HSCTM for evaluating the deformation mode and crushing force of a crash box specimen [23]

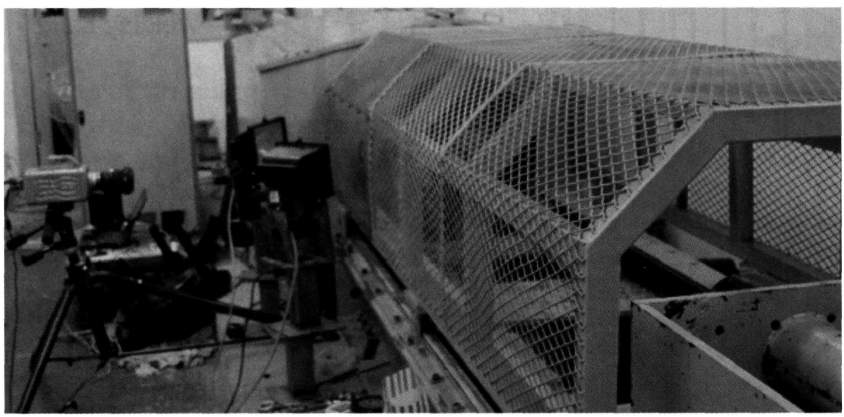

Figure 10. The high speed camera to capture the deformation of the specimen during the crushing test

The crushing force was sensed by the load cell and the force signal was sampled and recorded by using a data acquisition system. Pictures of the crushing process were captured by a high speed camera, as shown in Figure 10, at the rate of 5000 frames per second. The pictures were processed to obtain data of specimen displacements vs time. By synchronizing the initial impact times of the crushing forces and the displacements, the instantaneous force vs displacement curve was constructed. The curve was further processed to obtain the mean crushing force vs displacement curve.

Crash Box Specimens

Two specimens were prepared for the crushing tests, the single-walled and the double-walled square column. The double-walled column was built by inserting an inner square column inside an outer column having the dimensions similar to those of the single-walled column. The nominal width and height of the

single-walled square column are 46 mm and 180 mm, respectively. For the double-walled columns, the nominal width and height of the inner column are 27 mm and 180 mm, respectively. Each column was made from two rectangular 1 mm thick plates made of St37 mild steel which were bent into two U-profiles. The two profiles were then joined by continuous welding, as shown in Figure 11.

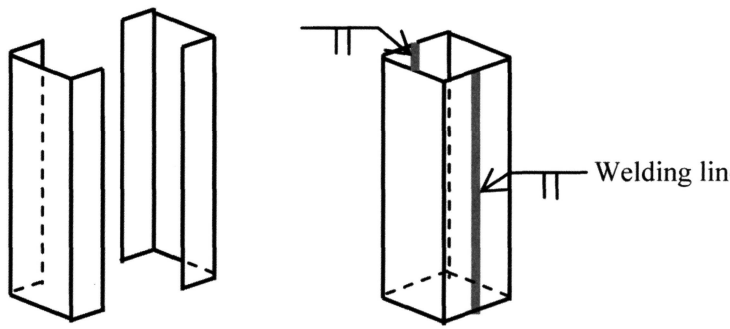

Figure 11. Preparation of a square column from two U-shaped profiles [21]

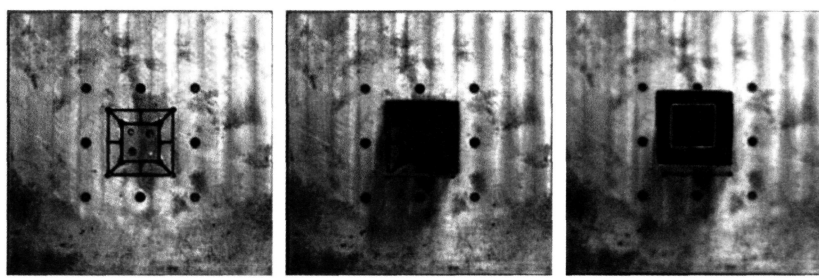

(a) (b) (c)

Figure 12. (a) The clamp, mounted with (b) single-walled and (c) double-walled columns

During the test, the specimen was mounted on a 25 mm thick clamp support which was attached to the HSCTM. One end of the specimen was inserted to 15 mm deep slots on the clamp support. The boundary conditions of the specimens were idealized as clamped-free ends. Figure 12 shows the clamp without and with the specimen, and Figure 13 shows a crushed specimen at the end of a test.

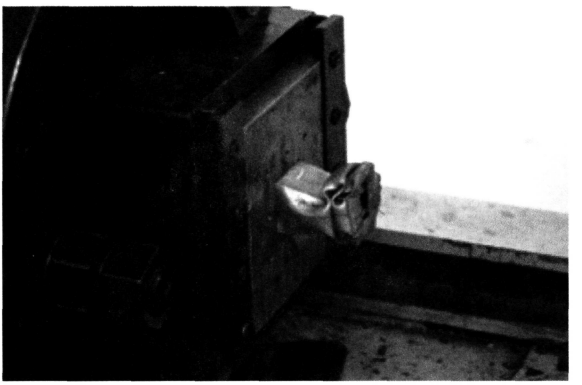

Figure 13. The specimen after the crushing test

Results of Crushing Tests

The single-walled column was crushed by the carrier at a speed of 3.74 m/s (kinetic energy of 2.03 kJ). The double-walled cell was crushed by the carrier at a velocity of 5.31 m/s (kinetic energy of 4.09 kJ). Figure 14 shows the deformation modes of the single and double-walled column. The deformation modes of both column are similar, in which two opposite sides of the column fold inward and the other two fold outward. Figure 15 shows the measured instantaneous crushing forces of the single and the double-walled columns. It can be seen that the force needed to crush the column has several peaks which relates to the formation of the folds of the specimen. The results also show that the crushing force of the double-walled columns is higher than that of the single-walled column.

The mean crushing force (P_m) is calculated from the energy absorbed by the crash box, or the area under the instantaneous force vs displacement curve, divided by the displacement:

$$P_m(\delta) = \frac{1}{\delta}\int_0^{\delta} P(x)dx \tag{1}$$

where P: instantaneous crushing force, δ: axial deformation of the column.

The P_m of each column, as shown in Figure 15, contains one peak in the begining that relates to the formation of the first fold, followed by a sloping curve approaching a constant value. For the single-walled column, P_m = 14.84 kN, δ (deformation) = 106.1 mm, and E_a (absorbed energy) =1.57 kJ. For the double-walled column, P_m = 27.93 kN, δ = 117.6 mm, and E_a = 3.28 kJ. Only 80% of impactor's kinetic energy is absorbed by the crash box. The remaining kinetic energy at the latest stage of the crushing process in the form

(a) (b)

Figure 14. Deformation modes of (a) single-walled and (b) double-walled column

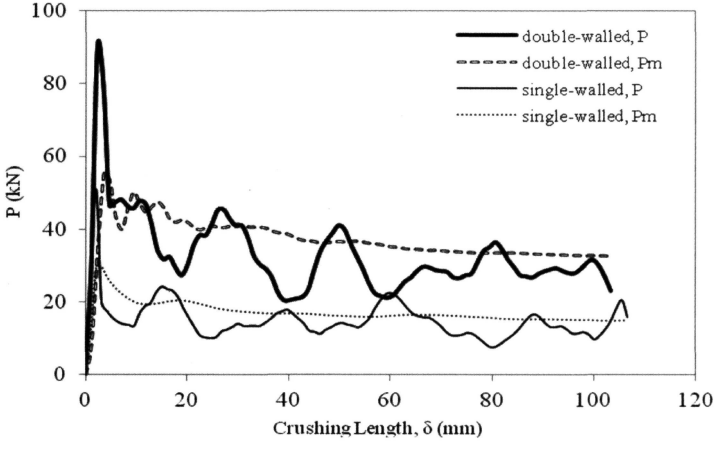

Figure 15. Instantaneous and mean crushing forces of the columns

of the motions of the impactor, the specimen, and the clamp, was absorbed by the HSCTM damper.

The P_m of the double-walled column is almost twice the P_m of the single-walled column despite the fact that the double-walled column is built by adding an inner column with smaller cross section. Yuen et al. [20] also observed this behavior where they did quasi-static experiments on two single- walled columns separately and on a double-walled column built from the two single-walled

columns. They found that the crushing force of the double-walled column is slightly higher than the added crushing forces of the inner and outer-columns separately. They predicted that the interaction between the inner and outer-column provides the extra resistive crushing force.

Finite Element Simulations

The data obtained from the tensile tests and the crushing tests were used in the numerical simulations of the axial impact of the columns using explicit finite element software package. Two main parts of the finite element model are the impactor that represents the carrier and the column. The velocity and mass of the impactor were set to be the same as those in the experiment.

The column was modeled using 1 mm × 1 mm quadrilateral Belytschko–Tsay four-nodes shell elements, while the impactor was modeled using hexahedral eight-node solid rigid elements, as shown in Figure 16. To simulate the clamp condition during the experiment, the column model was constrained at nodes from the lower end up to 15 mm above it. The impactor was allowed to move only in longitudinal axis of the column.

The constitutive behavior of the thin-shell element for the column material was selected to be based on the elastoplastic material model with Von Mises's isotropic plastic algorithm. The stress-strain behavior was simulated as piecewise-linear plastic. The true stress vs effective plastic strain curves obtained from the tensile tests were used to describe the material properties

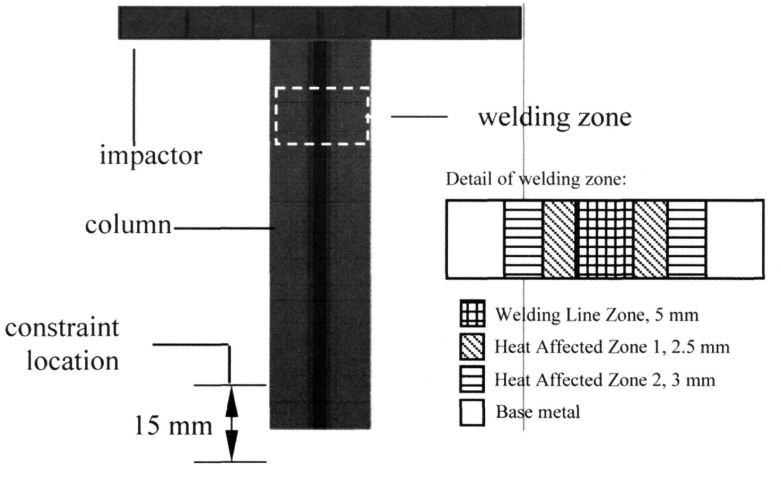

Figure 16. Finite element model of the column subjected to axial impact loading

of the column. To make the model more realistic, the welding zone was divided into 3 groups: the welding line zone, the heat affected zone-1 (HAZ-1) and the heat affected zone-2 (HAZ-2) as shown in Figure 16. The flow stress of the material at each zone was set to be proportional to that of the base metal by multiplying it to a factor that depends on the hardness ratio, i.e. the ratio of hardness of each area to that of the base metal. Fom Vickers micro-hardness test results, the hardness ratios of the welding line, the HAZ-1 and the HAZ-2 are respectively 2.14, 1.41, and 1.16.

The detailed finite element modeling and analysis can be found in [21]. To evaluate the effect of material modeling to the crushing force of the crash box, analyses that based on the quasi-static material properties only were carried out as well.

Results of Finite Element Simulations

Figure 17 shows the deformation modes of the columns obtained from the numerical simulations and the crushing tests. It can be seen that the finite element analysis can predict the deformation modes quite well.

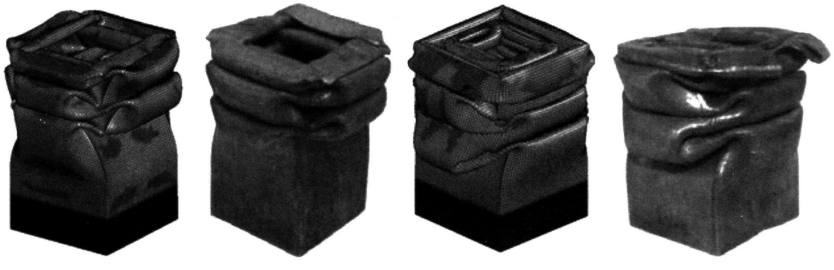

(a) (b) (c) (d)

Figure 17. Comparisons between the numerical and experimental deformation modes of the single-walled column (a , b) and of the double-walled column (c, d)

Figure 18 shows the instantaneous and the mean crushing forces of the single-walled column obtained from FEM simulations using only the quasi-static and the strain-rate dependent material data. It can be seen that the simulations employing the strain-rate material data can predict crushing forces that are close enough to the experiment result. Similar agreements can be observed for double-walled column as shown in Figure 19. The use of strain-rate dependent material data in the finite element simulations improves the predictions of the crushing force of the column.

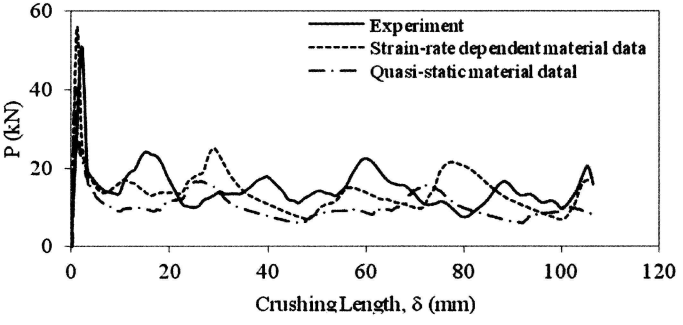

(a)

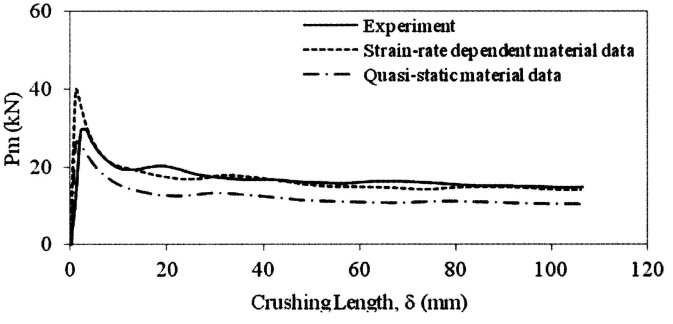

(b)

Figure 18. Comparison of (a) the crushing force and (b) the mean crushing force of the single-walled column obtained from FEM simulations and experiment

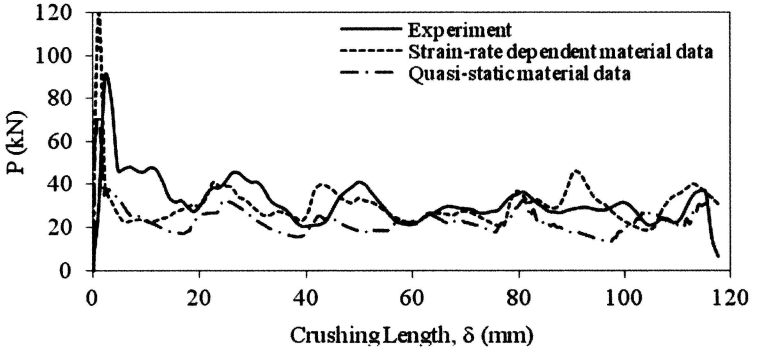

(a)

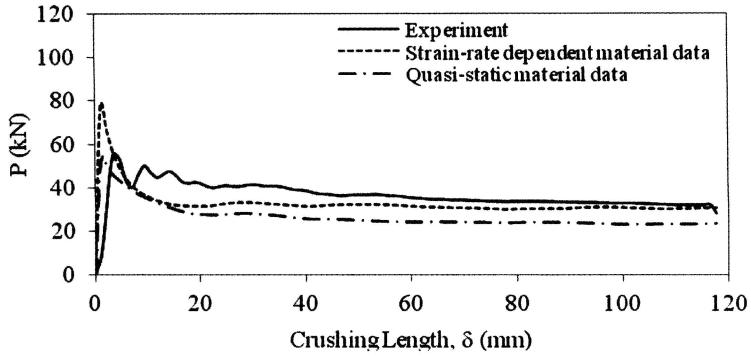

(b)

Figure 19. Comparison of (a) the crushing force and (b) the mean crushing force of the double-walled column obtained from FEM simulations and experiment

Conclusion

Experiments to support and validate the numerical simulations of axially crushed single and double-walled columns have been performed successfully.

The measurement of the material properties at several strain-rates provided stress-strain curves of the St37 mild steel which show strain-rate sensitivity. At the quasi-static strain-rate, the Young's modulus of the material is 197 GPa which is within the normal range for steel. The yield and ultimate strengths of the material are slightly lower than those found from the data-sheet of the St37 mild steel. At higher strain-rates, the yield and ultimate strengths of the material increase noticeably.

Results of the axial crushing tests show that the crushing force of the double-walled square column which comprises an inner and an outer columns is almost twice the crushing force of the outer column, or higher than the sum of crushing forces of the inner and the outer column separately. These results are in agreement with experimental results conducted by other researcher.

The finite element analysis using the strain-rate sensitive material data is able to predict the crushing forces and deformation modes of the columns which are in good agreement with those obtained from the crushing tests.

Acknowledgement

The research is funded by The Directorate General of Higher Education of Republic of Indonesia under the scheme of International Research Collaboration

and Scientific Publication 2012, and is supported by CSMD Laboratory of Korea Advanced Institute of Science and Technology, South Korea, which are gratefully acknowledged.

References

[1] Hou, S., Li, Q. and Long, S. (2006). "Optimization of beam section with crashworthiness criterion based on the explicit finite element technology," Journal on Numerical Method and Computer Applications, 27(4), 271-280.

[2] Alexander, J. M. (1960). "An approximate analysis of the collapse of thin cylindrical shells under axial loading," The Quarterly Journal of Mechanics and Applied Mathematics 13(1), 10-15.

[3] Wierzbicki, T. and Abramowicz, W. (1983). "On the crushing mechanics of thin-walled structures," Journal of Applied Mechanics, 50(4a), 727-734.

[4] Abramowicz, W. and Wierzbicki, T. (1984). "Dynamic axial crushing of square tubes," Int. J. of Impact Engineering, 2(2), 179-208.

[5] Andrews, K. R. F., England, G. L. and Ghani, E. (1983). "Classification of the axial collapse of cylindrical tubes under quasi-static loading," International Journal of Mechanical Science, 25(9-10), 687-696.

[6] Abramowicz, W. and Wierzbicki, T. (1989). "Axial crushing of multi corner sheet metal columns," Journal of Applied Mechanics 56(1), 113-120.

[7] Langseth, M. and Hopperstad, O. S. (1996). "Static and dynamic axial crushing of square thin-walled aluminium extrusions," International Journal of Impact Engineering 18(7-8), 949-968.

[8] Langseth, M., Hopperstad, O. S. and Hanssen, A. G. (1998). "Crash behaviour of thin-walled aluminium members," Thin-Walled Structures 32(1-3), 127-150.

[9] Langseth, M., Hopperstad, O. S. and Berstad, T. (1999). "Crashworthiness of aluminum extrusions: Validation of numerical simulation, effect of mass ratio and impact velocity," Int. J. of Impact Engineering 22(9-10), 829-854.

[10] Sun, J. and Osire, S. E. (2002). "Prediction of energy absorption of thin tubes," Proceeding of ASME GSTC, 63-67.

[11] Rossi, A., Fawaz, Z. and Behdinan, K. (2005). "Numerical simulation of the axial collapse of thin-walled polygonal section tubes," Thin-Walled Structures, 43(10), 1646-1661.

[12] Zhang, X. and Huh, H. (2010). "Crushing analysis of polygonal columns and angle elements," Int. J. of Impact Engineering, 37(4), 441-451.

[13] Tarigopula, V., Langseth, M., Hopperstad, O. S. and Clausen, A. H. (2005). "An experimental and numerical study of energy absorption in thin-walled

high-strength steel sections," WIT Transactions on Engineering Sciences 49, 495-507.

[14] Tarigopula, V., Langseth, M., Hopperstad, O. S. and Clausen, A. H. (2006). "Axial crushing of thin-walled high-strength steel sections," Int. J. of Impact Engineering, 32(5), 847-882.

[15] Aljawi, A. A. N., Abd-Rabou, M. and Asiri, S. (2004). "Finite element and experimental analysis of square tubes under dynamic axial crushing," European Congress on Computational Methods in Applied Sciences and Engineering.

[16] Zhang, X. W., Su, H. and Yu, T. X. (2009). "Energy absorption of an axially crushed square tube with a buckling initiator," Int. J. of Impact Engineering, 36(3), 402-417.

[17] Song, J., Chen, Y. and Lu, G. (2012). "Axial crushing of thin-walled structures with origami patterns," Thin Walled Structures, 54, 65-71.

[18] Huh, H., Kim, S. B., Song, J. H. and Lim, J. H. (2008). "Dynamic tensile charac-teristics of TRIP-type and DP-type steel sheets for an auto-body," International Journal of Mechanical Sciences, 50, 918-931.

[19] Huh, H., Song, J. H. and Lee, H. J. (2012). "Dynamic hardening equation of the auto-body steel sheet with the variation of temperature," Int. J. Automotive Technology, 13(1), 43-60.

[20] Yuen, S. C. K., Nurick, G. N. and Starke, R. A. (2008). "The energy absorption characteristics of double-cell tubular profiles," Latin American Journal of Solids and Structures, 5, 289-317.

[21] Jusuf, A., Dirgantara, T., Gunawan, L. and Putra, I. S. (2012). "Numerical and experimental study of single-walled and double-walled columns under dynamic axial loading," Journal of Mechanical Engineering, 9(2), 53-72.

[22] High Strain Rate Experts Group, (2005). "Recommendation for Dynamic Tensile Test of Sheet Steels", International Iron and Steel Institute.

[23] Kim, S. B., Huh, H., Bok, H. H. and Moon, M. B. (2011). "Forming limit diagram of auto-body steel sheets for high-speed sheet metal forming," Journal of Materials Processing Technology, 211, 851-862.